January, 1987] *Bull. Chem. Soc. Jpn.*, ***60***, *111—117 (1987)*

The Phase Transition of 1,4-Dialkyl-1,4-diazoniabicyclo[2.2.2]octane Dibromides, C_n-DABCO-C_{n+1}-Br_2 ($10 \leqq n \leqq 17$)

Kengo Imamura, Takashi Nogami,* and Yasuhiko Shirota
Department of Applied Chemistry, Faculty of Engineering, Osaka University,
Yamadaoka, Suita, Osaka 565
(Received July 26, 1986)

The phase transitions of 1,4-dialkyl-1,4-diazoniabicyclo[2.2.2]octane dibromide (bis(quaternary alkyl bromide salts) of DABCO) in which the difference in the carbon numbers of the two alkyl groups is one, were studied on the basis of measurements of differential scanning calorimetry, infrared absorption spectroscopy, and bromide-anion conductivities. The DSC measurements showed that an endothermic transition occurred at T_{c1} when the sample was heated from room temperature. An exothermic transition occurred at T_{c2}($T_{c2}<T_{c1}$) when the sample was cooled after it had been heated above T_{c1}. The transition temperatures (T_{c1} and T_{c2}), the transition enthalpies, and the transition entropies increased as the increase in the alkyl-chain lengths. T_{c1} was found to be governed by the even numbers of the alkyl group. The temperature dependence of the IR absorption spectra showed that the *trans*-zigzag conformation of the alkyl chain was destroyed by a conformational change above T_{c1}, and that the annealed sample existed as a metastable phase. The temperature dependence of the bromide-anion conductivities showed abrupt increases in the conductivities by three orders of magnitude at around the transition temperatures. The temperatures of the conductivity jump of the virgin samples were usually higher than those of the annealed samples. The differences in these two temperatures tended to become smaller as the increase in the alkyl-chain lengths. This fact can be explained as that the solid-state properties of the unsymmetric bis(quaternary salts) of DABCO tend to resemble those of the symmetric bis(quaternary salts) of DABCO as the increase in the alkyl-chain lengths.

A series of 1,4-dialkyl-1,4-diazoniabicyclo[2.2.2]octane dihalides (denoted as bis(quaternary salts) of DABCO) were found to exhibit phase transitions above room temperature by us.[1–4] The phase transition was studied by means of a DSC, IR absorption spectra, and a study of halide-anion conductivities. The phase transition of the symmetric bis(quaternary salts) was quite different from that of the unsymmetric bis(quaternary salts). In the case of the symmetric salts, almost a reversible transition was observed.[1,2] On the other hand, the unsymmetric salts were converted to the metastable phase when they were heated above the transition temperature, and then cooled.[3,4] The thermodynamic properties of the unsymmetric salts were explained by free energy-temperature relation. Some of the unsymmetric salts showed the conversion from the metastable phase to the stable phase during several days when they were kept at room temperature. The larger the difference in the carbon numbers of the two alkyl groups attached to DABCO nitrogens, the faster was the conversion rate from the metastable phase to the stable phase.[4] When the difference in the carbon numbers of the two alkyl groups was two, the conversion rates were too slow to be followed.[3] If we designate the bis(quaternary alkyl halide salt) of DABCO by the halide anion and by the numbers of the alkyl carbons (see Refs. 3 and 4),[5] the thermodynamic properties of the symmetric salts, C_n-DABCO-C_n-X_2 (X=Cl, Br, and I; $10 \leqq n \leqq 22$),[1,2] are quite different from those of the unsymmetric salts, C_n-DABCO-C_{n+2}-Br_2 ($10 \leqq n \leqq 16$)[3] and C_{10}-DABCO-C_n-Br_2 ($13 \leqq n \leqq 22$).[4] Thus, the phase transitions of a series of the unsymmetric salts, C_n-DABCO-C_{n+1}-Br_2, are interesting, because they seem to belong to the borderline of the different behaviors of the phase transitions. We studied the phase transitions of the bis(quaternary alkyl bromide salts) of DABCO, C_n-DABCO-C_{n+1}-Br_2 ($10 \leqq n \leqq 17$), by means of DSC, IR absorption spectra, and the measurements of the bromide-anion conductivities. The materials studied are shown in Fig. 1.

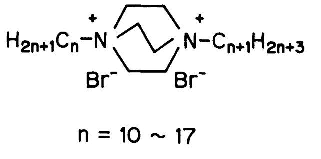

Fig. 1. Unsymmetric bis(quaternary alkyl bromide salts) of DABCO, C_n-DABCO-C_{n+1}-Br_2.

Experimental

Syntheses of Unsymmetric Bis(quaternary salts) of DABCO. The unsymmetric salt of DABCO was synthesized by two steps of the reactions, i.e., a synthesis of the mono(quaternary salt) by the reaction of DABCO with an equimolar amount of alkyl bromide, followed by a reaction of the resultant mono(quaternary salt) with another alkyl bromide. Detailed procedures were described previously.[3,4] All of the materials were recrystallized four or five times. The solvents of the recrystallization are acetonitrile for C_n-DABCO-C_{n+1}-Br_2 ($10 \leqq n \leqq 14$) and ethanol for C_n-DABCO-C_{n+1}-Br_2 ($15 \leqq n \leqq 17$) respectively.

Measurements. The DSC, the bromide-anion conductivities, and the IR absorption spectra were measured by the methods described previously.[2–4]

Results and Discussion

DSC Measurements. The DSC measurements were made while changing the temperature by 5 °C min^{-1}. When virgin samples$^{6)}$ were heated from room temperature, endothermic signals ($\Delta H_{en,1}$) were obtained at T_{c1}. C_{11}–DABCO–C_{12}–Br_2 and C_n–DABCO–C_{n+1}–Br_2 (n=10, 13, and 15) showed three and two endothermic signals respectively. On the other hand, C_n–DABCO–C_{n+1}–Br_2 (n=12, 14, 16, and 17) showed only one endothermic signal. When the samples were cooled after they had once been heated above T_{c1}, all of them showed one exothermic signal ($\Delta H_{ex,1}$) at T_{c2} which was lower than T_{c1}; $T_{c1}>T_{c2}$. The succeeding heating-cooling cycles showed reproducible endothermic ($\Delta H_{en,2}$) and exothermic ($\Delta H_{ex,1}$) signals at around T_{c2}. The absolute values of $\Delta H_{ex,1}$ and $\Delta H_{en,2}$ were equal within the experimental error. Figure 2 shows the observed thermogram of C_{10}–DABCO–C_{11}–Br_2 as a typical example. The endothermic signals $\Delta H_{en,1}$ were usually broader$^{7)}$ than $\Delta H_{en,2}$ for all of the materials studied. The observation of at least two transition temperatures (T_{c1} and T_{c2}) can be explained by the free energy-temperature relation as described before.$^{3,4)}$ According to this, the sample exists as a metastable phase (C_M) when it is heated above T_{c1} and then cooled. Even if the sample was left at room temperature for weeks after it had been heated above T_{c1}, it showed endothermic ($\Delta H_{en,2}$) and exothermic ($\Delta H_{ex,1}$) signals at around T_{c2}. This fact shows that the potential barrier from the C_M phase to the stable phase (C_L) is too high for the C_M phase to go back to the C_L phase. Similar phenomena were also observed for C_n–DABCO–C_{n+2}–Br_2 ($10 \leqq n \leqq 16$).$^{3)}$ This is consistent with the previous observation$^{3,4)}$ that the conversion rate from C_M to C_L becomes slower as the decrease in the differences in the carbon numbers of the two alkyl chains attached to DABCO nitrogens. Part of Table 1 shows some materials, T_{c1}, T_{c2}, $\Delta H_{en,1}$,$^{8)}$ ΔS_1 ($=\Delta H_{en,1}/T_{c1}$),$^{8)}$ $\Delta H_{en,2}$, and ΔS_2 ($=\Delta H_{en,2}/T_{c2}$). Here ΔS_1 and ΔS_2 denote the transition entropies at T_{c1} and T_{c2} respectively. Since the virgin samples of C_n–DABCO–C_{n+1}–Br_2 (n=10, 11, 13, 15) showed more than one transitions, all of the transition temperatures and the corresponding transition enthalpies and transition entropies are shown for these materials in this table. The transition temperatures were obtained by the onsets of the endothermic signals. Figure 3 plots the transition temperatures (T_{c1} and T_{c2}) against the carbon numbers (n) of the alkyl groups of C_n–DABCO–C_{n+1}–Br_2. The transition temperatures of the symmetric salts, C_n–DABCO–C_n–Br_2 and C_{n+1}–DABCO–C_{n+1}–Br_2,$^{2)}$ are also plotted for the sake of comparison. The following characteristics can be seen from Fig. 3. (1) The transition temperatures tend to increase as the increase in the alkyl-chain length. (2) The separation between T_{c1} and T_{c2} becomes smaller as the increase in the alkyl-chain length. (3)

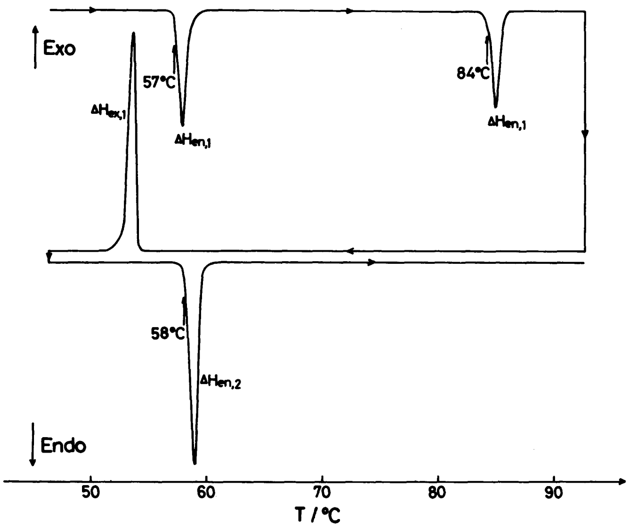

Fig. 2. DSC thermogram of C_{10}–DABCO–C_{11}–Br_2. Note that the sum of the two endothermic heats of transition ($\Delta H_{en,1}$) is close to the value of $\Delta H_{en,2}$.

Table 1. Materials, and the Transition Temperatures, Transition Enthalpies, Transition Entropies, and the Ratios of the Bromide-Anion Conductivities Before and After the Transitions

Materials	T_{c1} / °C	$\Delta H_{en,1}$ / kJ mol^{-1}	ΔS_1 / J/(mol deg)	$\sigma_h/\sigma_1$$^{a)}$	T_{c2} / °C	$\Delta H_{en,2}$ / kJ mol^{-1}	ΔS_2 / J/(mol deg)	$\sigma_h/\sigma_1$$^{b)}$
C_{10}–DABCO–C_{11}–Br_2	57, 84	27.1, 22.6	82, 63	820, 4$^{c)}$	58	48.9	148	1900
C_{11}–DABCO–C_{12}–Br_2	69, 77, 82	16.2, 22.7, 25.8	47, 65, 73	4500	65	51.7	153	2100
C_{12}–DABCO–C_{13}–Br_2	77	62.3	178	6000	72	59.7	173	5800
C_{13}–DABCO–C_{14}–Br_2	86, 87	69.3	193	1600	78	68.0	194	1500
C_{14}–DABCO–C_{15}–Br_2	88	76.9	213	1000	83	76.1	214	3200
C_{15}–DABCO–C_{16}–Br_2	89, 91	78.7	217	3300	87	78.4	218	3200
C_{16}–DABCO–C_{17}–Br_2	92	85.7	235	1700	90	87.3	240	1800
C_{17}–DABCO–C_{18}–Br_2	92	90.2	247	3100	92	96.1	263	1800

a) For the virgin samples. b) For the annealed samples. c) As shown in Fig. 6, two steps of the conductivity jumps were observed.

T_{c1}'s of C_n-DABCO-C_{n+1}-$Br_2$⁹⁾ are close to either the corresponding transition temperatures of C_n-DABCO-C_n-Br_2 or those of C_{n+1}-DABCO-C_{n+1}-Br_2. It is noteworthy that T_{c1}'s of C_n-DABCO-C_{n+1}-Br_2 (n= odd number) and those of C_n-DABCO-C_{n+1}-Br_2 (n=even number) are close to the transition temperatures of C_{n+1}-DABCO-C_{n+1}-Br_2 and C_n-DABCO-C_n-Br_2 respectively.¹⁰⁾

The characteristic (1) above can be explained as follows. Since the phase transition is caused mainly by a conformational change in the alkyl groups,²⁻⁴⁾ a parallel relation between the transition temperature and the alkyl-chain length arises from an increase in the van der Waals force between molecules as the increase in the alkyl-chain length. The characteristic (2) can be explained as follows. The molecular shape of the unsymmetric bis(quaternary salt) of DABCO tends to resemble that of the symmetric salt as the increase in the alkyl-chain length. Thus, C_{17}-DABCO-C_{18}-Br_2 showed reversible transition (only one transition temperature) like the cases of the symmetric bis(quaternary alkyl halide salts) of DABCO.¹˒²⁾ Although the characteristic (3) is interesting, the reason is as yet not clear. Since the present materials possess both even and odd numbers of the alkyl carbons, the following expression (3)′ is simpler for the characteristic (3). (3)′ The transition temperature (T_{c1}) of C_n-DABCO-C_{n+1}-Br_2 is determined by the alkyl group of the even numbers of carbons, and it is close to that of the corresponding symmetric salt possessing the same (even) number of alkyl carbons.

Figure 4 plots the transition enthalpies ($\Delta H_{en,1}$ and $\Delta H_{en,2}$) against the carbon numbers (n) of the alkyl groups of C_n-DABCO-C_{n+1}-Br_2. This figure also shows similar plots of the transition enthalpies of the symmetric bis(quaternary salts),²⁾ C_n-DABCO-C_n-Br_2 and C_{n+1}-DABCO-C_{n+1}-Br_2, for the sake of comparison. The dotted circles of C_n-DABCO-C_{n+1}-Br_2 (n=10, 11) mean the sums of the transition enthalpies ($\Delta H_{en,1}$) of these materials. The following three characteristics can be seen from Fig. 4. (1) Both $\Delta H_{en,2}$ and $\Delta H_{en,1}$ tend to increase as the increase in the alkyl-chain length. (2) $\Delta H_{en,1}$'s are close to $\Delta H_{en,2}$'s for

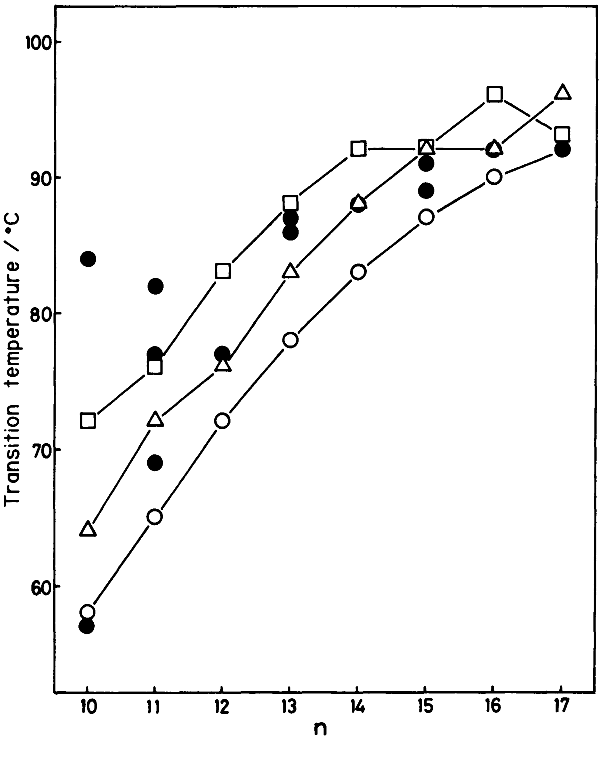

Fig. 3. The plot of the transition temperatures (T_{c1} and T_{c2}) against the carbon numbers (n) of alkyl group of C_n-DABCO-C_{n+1}-Br_2. The transition temperatures of the symmetric salts, C_n-DABCO-C_n-Br_2 and C_{n+1}-DABCO-C_{n+1}-Br_2, are also plotted for the sake of comparison.

●: T_{c1} of C_n-DABCO-C_{n+1}-Br_2, ○: T_{c2} of C_n-DABCO-C_{n+1}-Br_2. △: T_c of C_n-DABCO-C_n-Br_2, □: T_c of C_{n+1}-DABCO-C_{n+1}-Br_2.

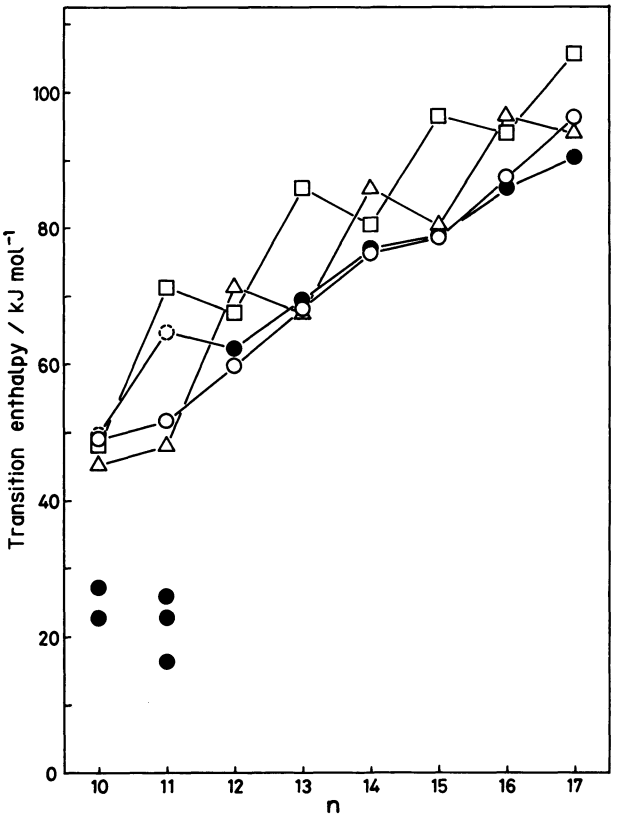

Fig. 4. The plot of the transition enthalpies ($\Delta H_{en,1}$ and $\Delta H_{en,2}$) against the carbon numbers (n) of alkyl group of C_n-DABCO-C_{n+1}-Br_2. The transition enthalpies of the symmetric salts, C_n-DABCO-C_n-Br_2 and C_{n+1}-DABCO-C_{n+1}-Br_2, are also plotted for the sake of comparison. Dotted circles mean the sum of the two transition enthaplies ($\Delta H_{en,1}$)for C_{10}-DABCO-C_{11}-Br_2 and that of the three transition enthalpies ($\Delta H_{en,1}$) for C_{11}-DABCO-C_{12}-Br_2.

●: $\Delta H_{en,1}$ of C_n-DABCO-C_{n+1}-Br_2, ○: $\Delta H_{en,2}$ of C_n-DABCO-C_{n+1}-Br_2. △: ΔH of C_n-DABCO-C_n-Br_2, □: ΔH of C_{n+1}-DABCO-C_{n+1}-Br_2.

C_n-DABCO-C_{n+1}-Br_2 ($12 \leqq n \leqq 17$). In the case of C_{10}-DABCO-C_{11}-Br_2, the sum of the two transition enthalpies ($\Delta H_{en,1}$) is close to $\Delta H_{en,2}$ (see also Fig. 2). (3) Comparison of $\Delta H_{en,2}$'s with the transition enthalpies of the symmetric salts gives the following rules: $\Delta H_{en,2}$'s of C_n-DABCO-C_{n+1}-Br_2 (n=odd number) are close to the transition enthalpies of the corresponding symmetric salts, C_n-DABCO-C_n-Br_2; if n is an even number, the following order holds except for C_{10}-DABCO-C_{11}-Br_2 (ΔH for C_n-DABCO-C_n-Br_2>ΔH for C_{n+1}-DABCO-C_{n+1}-Br_2>$\Delta H_{en,2}$ for C_n-DABCO-C_{n+1}-Br_2). Figure 5 plots the transition entropies (ΔS_1 and ΔS_2) against the carbon numbers (n) of the alkyl group of C_n-DABCO-C_{n+1}-Br_2. This figure also shows similar plots of the transition entropies of the symmetric bis(quaternary salts),[2,3] C_n-DABCO-C_n-Br_2 and C_{n+1}-DABCO-C_{n+1}-Br_2, for the sake of comparison. The dotted circles of C_n-DABCO-C_{n+1}-Br_2 (n=10, 11) mean the sum of the transition entropies (ΔS_1) of these materials. From Fig. 5, the characteristics (1)—(3) above of the transition enthalpies also hold in the cases of the transition entropies. From the Boltzmann relation, $\Delta S=R \ln W$, the numbers of sites (W) above the transition temperatures were estimated to be in the range of 300—5.7×10^{13} for the virgin and the annealed samples.[6,11] The large values of W suggest that the conformational change occurs at the every carbon site of the alkyl groups.

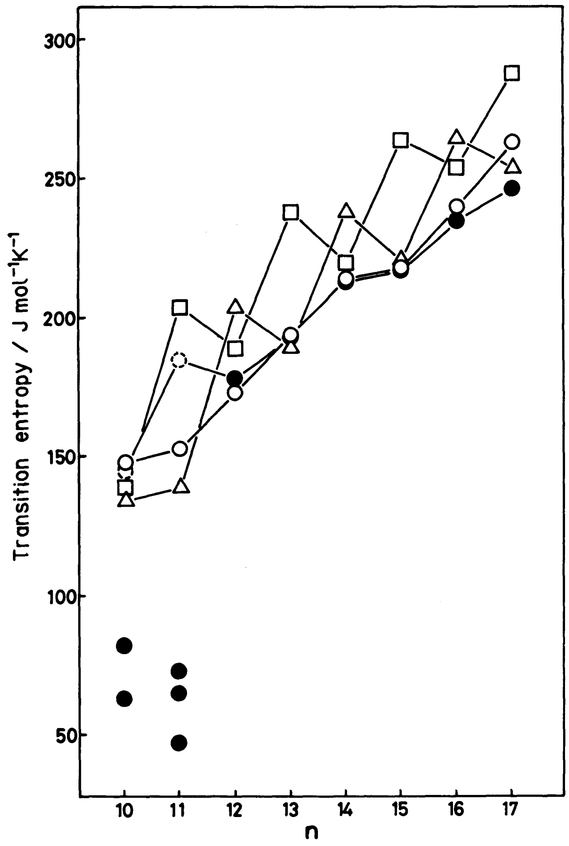

Fig. 5. The plot of the transition entropies (ΔS_1 and ΔS_2) against the carbon numbers (n) of alkyl group of C_n-DABCO-C_{n+1}-Br_2 ($\Delta S_1=\Delta H_{en,1}/T_{c1}$, $\Delta S_2=\Delta H_{en,2}/T_{c2}$). The transition entropies of the symmetric salts, C_n-DABCO-C_n-Br_2 and C_{n+1}-DABCO-C_{n+1}-Br_2, are also plotted for the sake of comparison. Dotted circles mean the sum of the two transition entropies for C_{10}-DABCO-C_{11}-Br_2 and that of the three transition entropies for C_{11}-DABCO-C_{12}-Br_2 respectively.
●: ΔS_1 of C_n-DABCO-C_{n+1}-Br_2, ○: ΔS_2 of C_n-DABCO-C_{n+1}-Br_2. △: ΔS of C_n-DABCO-C_n-Br_2, □: ΔS of C_{n+1}-DABCO-C_{n+1}-Br_2.

The characteristic (1) for the transition enthalpies is explained by the increase in the van der Waals force between molecules as the increase in the alkyl-chain length. The characteristic (1) for the transition entropies could be explained as follows. Since the phase transition is mainly caused by a conformational change in the alkyl group, the number of the sites after the transition increase as the increase in the alkyl-chain length. This gives rise to an increase in the transition entropies as an increase in the alkyl-chain length. The characteristic (2) for the transition enthalpies and entropies suggests that the structure of the C_M phase is not very different from that of the C_L phase. Since the difference in the numbers of the alkyl carbons is one in the present materials, their thermodynamic properties resemble those of the symmetric salts which have shown no clear indication of the presence of the metastable phase. The characteristic (2) is in common with the cases of the unsymmetric salts, C_n-DABCO-C_{n+2}-Br_2,[3] but is in sharp contrast to the cases of the unsymmetric salts, C_{10}-DABCO-C_n-Br_2.[4] In the latter cases, $\Delta H_{en,1}$ and ΔS_1 were larger than $\Delta H_{en,2}$ and ΔS_2 respectively. These facts show that the structural difference between C_L and C_M is small for C_n-DABCO-C_{n+1}-Br_2 and C_n-DABCO-C_{n+2}-Br_2, and that it tends to become larger with an increase in the alkyl-chain length. It is noteworthy that the sum of the two transition enthalpies ($\Delta H_{en,1}$) and that of the two transition entropies (ΔS_1) are close to $\Delta H_{en,2}$ and ΔS_2, respectively, in C_{10}-DABCO-C_{11}-Br_2. However, these relations do not hold in the case of C_{11}-DABCO-C_{12}-Br_2; the sums of the transition enthalpies and the transition entropies are larger than $\Delta H_{en,2}$ and ΔS_2 respectively. In order to clarify the thermodynamic properties described above, the determinations of the crystal structures of the present materials seem to be crucial.

Infrared Absorption Spectroscopy. The temperature dependence of the infrared absorption spectra of C_{13}-DABCO-C_{14}-Br_2 was measured as an example in order to obtain more information regarding the phase transition. It showed a similar change in the IR spectra as has been observed in the cases of the unsymmetric bis(quaternary alkyl bromide salts) of DABCO.[3,4] The virgin sample exhibited band progressions originating from 720 cm^{-1}. This is the evidence for the *trans*-zigzag conformation of the alkyl groups. The band progressions suddenly disappeared at T_{c1} when the sample was heated from room temperature, and they appeared again at T_{c2} upon cooling the sample. This fact shows that the *trans*-zigzag conformation of the alkyl group is destroyed in the high temperature phase, and that the annealed sample[6] exists as a metastable phase. This is consistent with the DSC results. The detailed

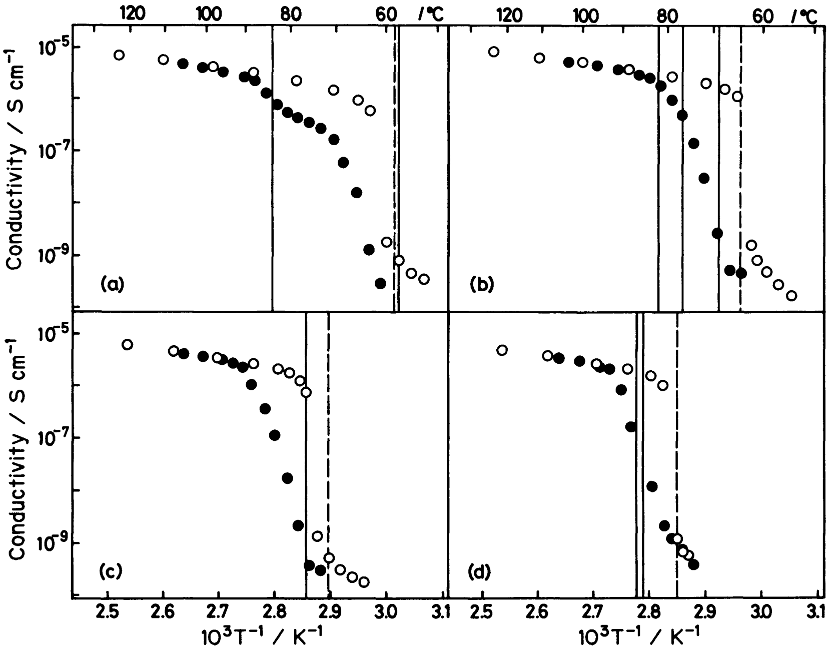

Fig. 6. Temperature dependence of the bromide-anion conductivities of C_n–DABCO–C_{n+1}–Br_2 ($10 \leqq n \leqq 13$) (●: virgin sample, ○: annealed sample). The vertical solid- and dotted-lines represent T_{c1} and T_{c2} respectively.
(a) $n=10$, (b) $n=11$, (c) $n=12$, (d) $n=13$.

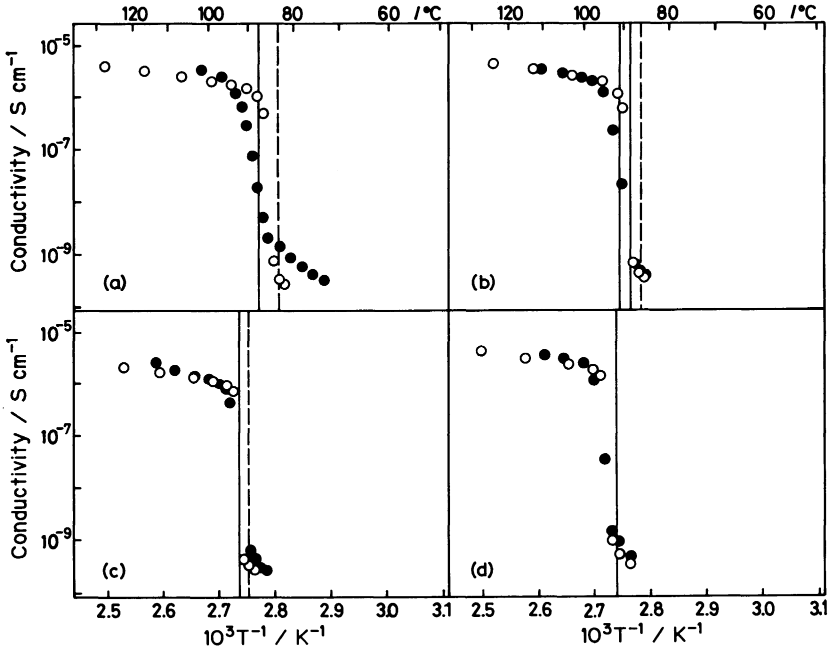

Fig. 7. Temperature dependence of the bromide-anion conductivities of C_n–DABCO–C_{n+1}–Br_2 ($14 \leqq n \leqq 17$) (●: virgin sample, ○: annealed sample). The vertical solid- and dotted-lines represent T_{c1} and T_{c2} respectively.
(a) $n=14$, (b) $n=15$, (c) $n=16$, (d) $n=17$.

discussion was given in the previous papers.[3,4]

Bromide-Anion Conductivities. All of the samples were confirmed to be bromide-anion conductors by the method described previously.[1] The bromide-anion conductivities were measured for the compressed pellet sample by an AC impedance method.[1–4] The conductivities of the virgin samples[6] were measured first by heating the sample slowly (0.5 °C min^{-1}) from room temperature across T_{c1}. The sample was then allowed to cool to room temperature, and the conductivities of the annealed sample[6] were measured by heating the sample again. Figures 6 and 7 show the temperature dependences of the bromide-anion conductivities of C_n–DABCO–C_{n+1}–Br_2 ($10\leqq n\leqq 13$) and C_n–DABCO–C_{n+1}–Br_2 ($14\leqq n\leqq 17$) respectively. Each figure shows both conductivities of the virgin and the annealed samples . The vertical solid- and dotted-lines represent T_{c1} and T_{c2} respectively. The conductivities less than 10^{-9} S cm^{-1} were below the limit of our measurements. All of the samples showed abrupt increases in the bromide-anion conductivities by three orders of magnitude at around the transition temperatures; the virgin and the annealed samples showed the conductivity jumps at around T_{c1} and T_{c2} respectively. Table 1 shows the ratios of the conductivities before (σ_l) and after (σ_h) the transition for the virgin and the annealed samples. They were found to be in the range of 1000 to 6000 for the virgin samples and in that of 1800 to 5800 for the annealed samples. The conductivity jump (σ_h/σ_l=6000) of C_{12}–DABCO–C_{13}–Br_2 is the largest of all of the materials studied hitherto.[2–4] To see closely Figs. 6 and 7, the following three characteristics are noteworthy. (1) The difference in the temperatures of the conductivity jumps between the virgin and the annealed samples tends to become smaller as the increase in the alkyl-chain lengths. (2) The conductivity jump becomes sharper as the increase in the alkyl-chain lengths. (3) Although the conductivities are quite different below the transition temperatures, they are almost similar above the transition temperatures with the activation energies of about 30 kJ mol^{-1}.

The characteristics (1) and (2) above are consistent with the results of the DSC measurements; the thermodynamic properties of the unsymmetric salts tend to resemble those of the symmetric salts as the increase in the alkyl-chain lengths. Since the symmetric salts showed only slight hysteresis of the conductivity jumps,[2] the characteristic (1) can be understood as a natural phenomenon. The characteristic (2) can also be deduced from the sharp conductivity jumps observed for the symmetric salts.[1,2] The characteristic (3) is a common phenomenon of all of the bis(quaternary alkyl halide salts) of DABCO, irrespective of the symmetric and unsymmetric salts, and it was discussed before.[2] From Figs. 6 and 7 and Table 1, it can not be said generally whether the virgin samples exhibit larger conductivity jumps than the annealed samples or not. The conductivity jump is caused by the formation of a large number of voids as a result of the conformational movement of the alkyl groups above the transition temperature.

Figures 6 and 7 also show the relations between the conductivity jumps and the transition temperatures (T_{c1} and T_{c2}). T_{c2}'s were located at the onsets of the conductivity jumps of the annealed samples except for C_{11}–DABCO–C_{12}–Br_2. T_{c1}'s were also located at the onsets of the conductivity jumps of the virgin samples for C_n–DABCO–C_{n+1}–Br_2(n=10, 11, 12, 17). However, T_{c1}'s were located at around the middle points of the conductivity jumps of the virgin samples for C_n–DABCO–C_{n+1}–Br_2(n=13, 14, 15, 16). The second T_{c1} of C_{10}–DABCO–C_{11}–Br_2 corresponds to the second conductivity jump. The second and the third T_{c1}'s of C_{11}–DABCO–C_{12}–Br_2 were located at around the end points of the conductivity jump. Although the complex behaviors of the relations between T_{c1}'s and the conductivity jumps are as yet not clear, they will reflect the difference in the formations of the voids as a result of the conformational change in the alkyl groups.

Summary. The phase transitions of bis(quaternary alkyl bromide salts) of DABCO, C_n–DABCO–C_{n+1}–Br_2 ($10\leqq n\leqq 17$), were studied by means of the DSC, the infrared absorption spectroscopy, and the measurements of the bromide-anion conductivities. As described in the Introduction, these materials seem to belong to the borderline of the solid-state properties between the symmetric and unsymmetric bis(quaternary salts) which have been studied previously.[1–4] As expected, the present materials showed both properties of the symmetric and the unsymmetric salts as will be shown below. (1) C_n–DABCO–C_{n+1}–Br_2 showed at least two transition temperatures (T_{c1} and T_{c2}), and the annealed samples were found to be converted to the metastable phase by the DSC and the IR absorption spectra. These properties are similar to the cases of the unsymmetric salts.[3,4] (2) The separation between T_{c1} and T_{c2} tends to become smaller with an increase in the alkyl-chain length. C_{17}–DABCO–C_{18}–Br_2, which has the longest alkyl groups of the present materials, showed only one transition temperature; this is similar to the cases of the symmetric salts.[1,2] These facts show that the thermodynamic properties of C_n–DABCO–C_{n+1}–Br_2 tend to resemble those of the symmetric salts as the increase in the alkyl-chain length. (3) T_{c1}'s are close to the transition temperatures of the corresponding symmetric salts. It is especially interesting that T_{c1} is governed by the alkyl group possessing even number of carbons. (4) $\Delta H_{cn,1}$'s and ΔS_1's are close to $\Delta H_{cn,2}$ and ΔS_2 respectively. These facts suggest that the structure of the metastable phase (C_M) is not very different from that of the low temperature phase (C_L). This is interesting in connection with the following observations; the symmetric salts did not show any presence of the C_M phase, but the unsymmetric salts showed C_M phase; when the difference in the carbon numbers of the two alkyl groups is larger than two, the structure of the C_M phase was assumed to be quite different from that of the C_L phase, unlike the cases of the present materials. Thus, C_n–DABCO–C_{n+1}–Br_2 can be said to possess intervening properties between the symmetric and unsymmetric salts. (5) The measurements of the bromide-anion conductivities revealed that conductivity jumps occurred at around T_{c1} and T_{c2} for the virgin and the annealed samples respectively. These phenomena are similar to the cases of the unsymmetric salts.[2,3] However, the differences in the two temperatures of the conductivity jumps tend to become smaller, and the conductivity jumps, themselves, tend to become sharper with an increase in the alkyl-chain lengths. These facts show that the temperature dependences of the bromide-anion conductivities tend to resemble those of the symmetric salts as the increase in the alkyl-chain lengths. The conductivity jump of C_{12}–DABCO–C_{13}–Br_2 was the largest of all of the materials studied hitherto.

We are grateful to Professor Shigekazu Kusabayashi and Dr. Shunsuke Takenaka, Faculty of Engineering, Osaka University, for the use of the DSC apparatus.

References

1) J. Shimizu, T. Nogami, and H. Mikawa, *Solid State Commun.*, **54**, 1009 (1985).

2) J. Shimizu, K. Imamura, T. Nogami, and H. Mikawa, *Bull. Chem. Soc. Jpn.*, **59**, 1443 (1986).

3) K. Imamura, J. Shimizu, and T. Nogami, *Bull. Chem. Soc. Jpn.*, **59**, 2699 (1986).

4) J. Shimizu, K. Imamura, T. Nogami, and H. Mikawa, *Bull. Chem. Soc. Jpn.*, **59**, 3367 (1986).

5) For example, 1-decyl-4-undecyl-1,4-diazoniabicyclo-[2.2.2]octane dibromide is abbreviated as C_{10}–DABCO–C_{11}–Br_2.

6) The virgin and the annealed samples mean the sample synthesized and the sample heated above T_{c1} at least once respectively.

7) The widths of all of the endothermic signals, $\Delta H_{en,2}$, were found to lie within 5 °C. However, those of the $\Delta H_{en,1}$ were broader than 5 °C, and are as follows: 5 °C and 5 °C, corresponding to two transitions for n=10; 11 °C, 8 °C, and 8 °C, corresponding to three transitions for n=11; 15 °C for n=12; 10 °C for n=13; 11 °C for n=14; 7 °C for n=15; 8 °C for n=16; 5 °C for n=17.

8) The two endothermic signals of C_n–DABCO–C_{n+1}–Br_2 (n=13, 15) were not separated well because of the proximity of the two transition temperatures. Thus, $\Delta H_{en,1}$'s were obtained by the total enthalpies of the two transitions, and ΔS_1 by dividing $\Delta H_{en,1}$ with the average transition temperatures (T_{c1}(average)=86.5°C for n=13, and T_{c1} (average)=90 °C for n=15).

9) The virgin samples of C_n–DABCO–C_{n+1}–Br_2 (n=11, 13, 15) possess more than one transition temperatures (T_{c1}). The second transition temperatures of these materials are close to the transition temperatures of the corresponding symmetric DABCO salts.

10) The characteristic (3) does not hold in the case of C_{10}–DABCO–C_{11}–Br_2. It showed large separation of the two transition temperatures (T_{c1}=57 °C, 84 °C).

11) The estimated numbers of sites (W) of C_n–DABCO–C_{n+1}–Br_2 above the transition temperatures are as follows. Virgin samples: 1.9×10^4 and 2000, corresponding to two transitions for n=10; 300, 2400, and 6200, corresponding to three transitions for n=11; 2×10^9 for n=12; 1.2×10^{10} for n=13; 1.3×10^{11} for n=14; 2.1×10^{11} for n=15; 1.8×10^{12} for n=16; 8.1×10^{12} for n=17. Annealed samples: 5.2×10^7 for n=10; 9.8×10^7 for n=11; 1.1×10^9 for n=12; 1.3×10^{10} for n=13; 1.5×10^{11} for n=14; 2.4×10^{11} for n=15; 3.7×10^{12} for n=16; 5.7×10^{13} for n=17.